A first-principles study of the Mechanical Stability and Electronic Properties of Lead-free Halide Inorganic Double Perovskites Cs_2InAgX_6 (X =F, Br, Cl, I)

Atarah, S. A.[1*], Gebreyesus, H. G.[1], and Egblewogbe, M. N. H[1]

[1]Department of Physics, University of Ghana, Legon, Ghana

***Corresponding author:** saatarah@ug.edu.gh

ABSTRACT

Lead-free double perovskites (DPs), Cs_2InAgX_6, specifically, were studied as candidate materials for photo voltaic cells (PVC). The density functional theory (DFT) methods as implemented in the Quantum Espresso suite was applied for the study. Equilibrium lattice parameters for the DP which are all face-centered cubic crystals, were determined as follows: a = 9.13 Å for X=F, a = 10.38 Å for X= Cl, a = 11.07 Å for X = Br and a = 11.39 Å for X = I. These findings align well with reported values. Additionally, elastic constants were calculated and found to be in fair agreement with reported values as well. Using the calculated elastic constants, all DPs were found to be ductile. The values of energy band gaps, Eg, calculated were Eg = 1.7 eV for X = F, Eg = 1.5 eV for X = Cl, Eg =0.9 for X = Br and Eg = 0.7 eV. It is noteworthy that, various studies, the experimentally reported Eg value for X = Cl, (in the range of 3.23-3.3 eV) significantly exceed the calculated Eg values in this work. The experimental Eg value for X = Cl as reported by several works is 3.23 - 3.3 eV, much higher than this and all calculated Eg values reported in this work. In summary, $Cs_2InAgCl_6$ emerges as a robust candidate material for PVCs, showcasing favorable mechanical stability and band gap characteristics. On the other hand, $Cs_2InAgBr_6$ would require band gap engineering to be a suitable material.

Keywords: Pb-free, halide double perovskite, photovoltaic cells, mechanical properties, first principles study

1.0 INTRODUCTION

Solar cell technology for harvesting energy is seen as a major source of energy for the future because it is eco-friendly and sustainable. The efficiency of solar cells has improved steadily over time as well (Nayak, P. K., Mahesh, S., Snaith, H. J., Cahen, 2019). It is also clear from the literature that Si based photovoltaic cells (PVCs) are by far the most successful technology for harvesting photovoltaic energy. However, power conversion efficiency (PCE) of Si based PVCs are rather low. Research for material alternatives to Si in solar cell and related technology is active and Perovskite materials are strong candidates for future PVC material due to their high laboratory PCE being reported. Perovskite materials have a general formula ABX_3, where A = monovalent cation, B = divalent, X is an anion, with

with commonly B = Pb. Pb-based halide perovskites have been studied extensively and are reported to hold promise for LED applications and for PVCs. They have been demonstrated to achieve power conversion efficiencies above 22%, and surpassing polycrystalline and thin-film silicon based PVCs (NREL, 2022). The features of perovskite material that lead to the high PCE are low carrier recombination, suitable absorption and extinction coefficients in the visible electromagnetic spectrum, high carrier mobility and direct energy band gap values (Mathew et al., 2019).

Optical, electronic and structural properties of various perovskite materials have been examined by many research groups both theoretically (D. Shi, V. Adinolfi, R. Comin, M. Yuan, E. Alarousu, A. Buin, Y. Chen & A. Rothenberger, 2015; J. H. Noh, S. H Im, J. H Heo, T. N Mandal, 2013; Meyer et al., 2018; Q. Dong, Y. Fang, Y. Shao, P. Mulligan, J. Qiu, L. Cao, 2015; S.D. Stranks, G.E. Eperon, G. Grancini, C. Menelaou, M.J. Alcocer, T. Leijtens & M. Herz, 2013; T.J. Jacobsson, M. Pazoki, A. Hagfeldt, 2015), and experimentally (Volonakis et al., 2017; W. Khan, S. Azam, M.B. Kanoun, 2016). Pb-based perovskite materials have been reported for their high PCE but Pb is toxic (Green et al., 2014), and environmentally hazardous when exposed to moisture which inevitably results from high humidity in the atmosphere (P.K. Kung, M.H. Li, P.Y. Lin, J.Y. Jhang, M. Pantaler, D.C. Lupascu, G. Grancini, 2020). Efforts are directed at minimizing or replacing Pb in PVCs. Therefore, the stability of Pb-free perovskites are being studied. An early attempt at realizing a Pb-free material was to replace Pb^{2+} with Sn^{2+} in the structure $APbX_3$ (X= Br, I, Cl). However such products were found to be unstable (Zhen Li, Mengjin Yang, Ji-Sang Park, Su-Huai Wei, Joseph J. Berry, 2016). Double perovskites are emerging as alternatives to the existing lead halide perovskites. The general formula for double perovskites is A_2BX_6 or $A_2BB'X_6$, where A and B are respectively inorganic cations and tetravalent ions with X a halide. Initial studies on double perovskites have reported mixed results. Combinations of Ag and Cu on one hand with Bi, In and Sn on the other in place of Pb^{2+} have been tried. Such products as Cs_2CuBiX_6 or $CsAgSnX_6$ were found to yield either indirect band gaps or energy band gaps larger than 2 eV(T.J. Jacobsson, M. Pazoki, A. Hagfeldt, 2015),(Volonakis et al., 2017)(Slavney, A. H.; Hu, T.; Lindenberg, A. M.; Karunadasa, 2016). Cs_2BiAgX_6 (X = Cl, Br) have been synthesized and found to exhibit band gaps in the visible range (Filip, M. R.; Hillman, S.; Haghighirad, A. A.; Snaith, H. J.; Giustino, 2016).

However, the band gaps of these compounds are indirect which is not ideal for applications in thin film photovoltaics. The study on $Cs_2AgBiBr_6$, by Savory et al reported an efficiency of less than 8% (Christopher N. Savory, Aron Walsh, 2016). W. Mukhtar et al (Waqas Mukhtar et al., 2021) using first principle studies reported that the double perov skites Rb_2NaInI_6 and Cs_2NaInI_6 are direct energy bandgaps of values 1.121 eV and 1.111 eV respectively.

Maughan et al (A.E. Maughan, A.M. Ganose, M.A. Almaker, D.O. Scanlon, 2018) and others (A. Kaltzoglou, D. Perganti, M. Antoniadou, A.G. Kontos, 2016) independently studied the Cs2SnI6 and reported an energy bandgap of nearly 1.2 eV) and carrier mobility of 509 cm2/V/ s. These reported band gap energies in the range of 1.0 eV are suitable for PVCs. Other promising double perovskites that are recommendable for use as active layers in PVCs are $Cs_2InSbCl_6$, $Cs_2AgInBr_6$, $Rb_2AgInBr_6$, and $Rb_2CuInCl_6$. Initial studies show that in addition to having desirable energy bandgaps, these have higher PCE compared to ABX_3 material (J. Zhou, J. Luo, X. Rong, P. Wei, M.S. Molokeev, Y. Huang, J. Zhao & X. Zhang, J. Tang, 2019; Michael M. Lee, Joël Teuschertsutomu, 2012; Xin-Gang Zhao, Dongwen Yang, Yuanhui Sun, Tianshu Li†, Lijun Zhang, Liping Yu, 2017). Although organic-inorganic compound combinations in perovskites have been used to implement optoelectronic devices, instability arising from long term expose to sunlight and humidity is reported as a factor to consider in adopting perovskites for PVC application (H.-S. Kim, C.-R. Lee, J.-H. Im, K.-B. Lee, T. Moehl, A. Marchioro & R. Humphry-Baker, J.-H. Yum, 2012), (Nam Joong Jeon, Jun Hong Noh, Woon Seok Yang, Young Chan Kim, Seungchan Ryu, 2015). The stability of perovskites is therefore a threat to their development as PVCs. Nishita et al (Mathew et al., 2019) presented preliminary results on the electronic and structural properties of Cs2InAgCl6 but the stability of the material was not reported. In this study, the mechanical stability of some lead–free double perovskite material (Cs_2InAgX_6; X= F, Cl, Br, I) was studied using DFT. Except $Cs_2InAgCl_6$, experimental data on which is being reported (Volonakis et al., 2017), the compounds with X = F, Br, and I are hypothetical but potentially represent an important class of promising PVC material. This study also discusses the electronic properties of the selected material.

2.0 METHODOLOGY AND COMPUTATIONAL DETAILS

For the current work, the Quantum Espresso (P Giannozzi, S Baroni, 2017) computational suite was used and the calculations were carried out using the plane wave DFT approach. The Perdew-Burke-Ernzerhof (PBE) Generalized Gradient Approximation (PBE-GGA) was applied. The electron exchange energy correlation functionals which were taken within the PBE formulation and ultrasoft pseudopotentials for solids (PBE-sol) were used to describe the atomic potentials. Indium 4d 5s orbitals were included for core correction whiles in general 4p 5s orbital were included for halides. For all calculations, the Hubbard +U correction was applied on Ag 3d orbital. The calculations did not include spin-orbital coupling effects as these have all The k-point meshes for all structures were generated according to Monkhorst-Pack scheme for the Brillouin zones. Sampling of Brillouin zone integration with k-point mesh 10×10×10 was set, while denser k-mesh of 12×12×12 was used for DOS calculations. The kinetic energy cut-off for electrons was determined by the minimum required for the element with the highest energy cut-off requirement and ranged between 60 Ry for Cs_2InAgI_6 and 90 Ry for $Cs_2InAgCl_6$. Stringent convergence requirements were set for each compound with interatomic force thresholds typically 10^{-7} Ry/Å. In all calculations the electron convergence threshold was 10^{-12} Ry. The equilibrium lattice parameters of crystals were computed by self consistently calculating the minimum total energy per unit cell of each compound for a range of values of lattice constants. A plot of energy vs volume was then fitted by the Birch-Murnaghan equation of state and the equilibrium lattice parameters (corresponding to minimum energy) obtained for each compound. Elastic constants were obtained directly from self consistent thermal computations. In order to predict the formation of stable perovskite the Goldschmidt test was used. As all the unit cells of the compounds were face centered cubic crystals, the bulk modulus, B, was obtained from the elastic constants C_{11}, C_{12} and C_{44} at zero pressure as:

$$B = \frac{C_{11} + 2C_{12}}{3} \quad (1)$$

The shear modulus G is taken as an average of the Voight (G_V) (Lv et al., 2016), Reuss (G_R) (Li et al., 2017) and Hill (Erum & Iqbal, 2016) approximations as

$$G = \frac{G_V + G_R}{2} (2)$$

where

$$G_R = \frac{5C_{44}(C_{11} - C_{12})}{4C_{44} + 3(C_{11} - C_{12})} (3)$$

and $G_V = \frac{C_{11} - C_{12} + 3C_{44}}{5} (4)$

The possibility of the selected atoms forming perovskite crystals stably was assessed by use of the Goldschmidt (Volonakis et al., 2017) tolerance (*t*) and octahedral (μfactors defined as

$$\mu = \frac{R_B}{R_X} (5)$$

$$t = \frac{R_{Cs} + R_X}{\sqrt{2}(R_B + R_X)} (6)$$

$$R_B = 0.5\left(R\left|\quad\right|+R_{Ag}\right)(7)$$

where R_{Cs}, R_X are the Shannon ionic radii of the Cs cation and the X anion respectively. R_B was estimated as the average of In and Ag ionic radii as shown in (7).

3.0 RESULTS

3.1 Structural properties and mechanical stability

Table 1 shows the calculated lattice and bulk constants, the octahedral and tolerance factors and the Pugh ratios for the material. Also included in the table are values from references. The calculated bulk moduli were reproduced by fitting to the energy-volume plot using the Birch-Murnaghan equation of state.

Table 1: Lattice constants, bulk and shear moduli and relate ratios of the perovskites

Anion X	**F**	**Cl**	**Br**	**I**
a (Å) This work	9.015	10.3897	10.8989	11.5385
a (Å) (References)	9.138 (M. Tariq, Malak Azmat Ali, A. Laref, 2020)	10.467 (Z. Zhou, M.S. Xia, X. Molokeev, D. Peng Zhang, 2017), 10.65 (Enamul Haque, 2019), 10.47 (expt. (Volonakis et al., 2017))	10.74 (Volonakis et al., 2017)	11.52(Hang Yin, Yeming Xian, Yongli Zhang, Wenzhe Li, 2019)
B (Gpa)	47.028	38.270, 29.12 (M. Tariq, Malak Azmat Ali, A. Laref, 2020), 46.8 (Enamul Haque, 2019)	23.465 23.46 (M. Tariq, Malak Azmat Ali, A. Laref, 2020)	109.970

G (Gpa)	13.77	14.828	23.465	364.669
Pugh ratio (= B / G)	3.415	2.580	3.103	0.290
octahedral factor, *t*	0.733	0.538	0.497	0.443
Tolerance, μ	0.985	0.937	0.925	0.909
Poisson ratio	1.347	0.328	0.352	0.3800

Table 2: Elastic constant and test of stability using elastic constants

Anion X	**F**	**Cl**	**Br**	**I**
C_{11} (GPa)	66.941	64.575, 93.03 (Enamul Haque, 2019)	131.205	204.390
C_{12} (GPa)	37.072	25.119, 23.69 (M. Tariq, Malak Azmat Ali, A. Laref, 2020)	43.632	62.764
C_{44} (GPa)	-13.045	12.231	15.038	20.542
$C_{11} > \lvert C_{12} \rvert$	Yes	Yes	Yes	Yes
$C_{44} > 0$	No	Yes	Yes	Yes
$C_{11} + C_{12} > 0$	Yes	Yes	Yes	Yes

Elastic constants hold information on the mechanical stability, the bonding, stiffness and other related properties of materials subjected to externally applied stress (Amal Moussali, Mahdad Benzardjab Amina, Benattou Fassi, Ibrahim Ameri, Mohammed Ameri, 2020). Table 2 shows the calculated elastic constants and the stability test results, whereas the calculated energy band gaps are shown in Table 3.

Table 3: Calculated energy band gaps (in eV) for the double perovskite material studied

Anion X	**F**	**Cl**	**Br**	**I**
This work	1.7	1.5	0.4	0.7
Other work (Theoretical)	3.44 (M. Tariq, Malak Azmat Ali, A. Laref, 2020)	1.5 (Volonakis et al., 2017), 1.35 (N.K. Noel, S.D. Stranks, A. Abate, C. Wehrenfennig, S. Guarnera & Petrozza, 2014),	0.58 (Z. Zhang, J. Su, J. Hou, Z. Lin, Z. Hu, J. Chang, J. Zhang, 2019), 1.33 (G. Volonakis, 2018), 1.5 (Xin-Gang Zhao, Dongwen Yang, Yuanhui Sun, Tianshu Li†, Lijun Zhang, Liping Yu, 2017)	0.76 (M. Tariq, Malak Azmat Ali, A. Laref, 2020)
Other work Experiment	-	3.3 (Volonakis et al., 2017), 3.23 (Slavney, A. H.; Hu, T.; Lindenberg, A. M.; Karunadasa, 2016)	-	-

The energy band structure displays fundamental electronic characteristics of a material. Figure 1 shows the energy band diagrams and the density of states (DoS) plot for the halide-based double perovskites studied whilst the projected density of states are shown in Figure 2.

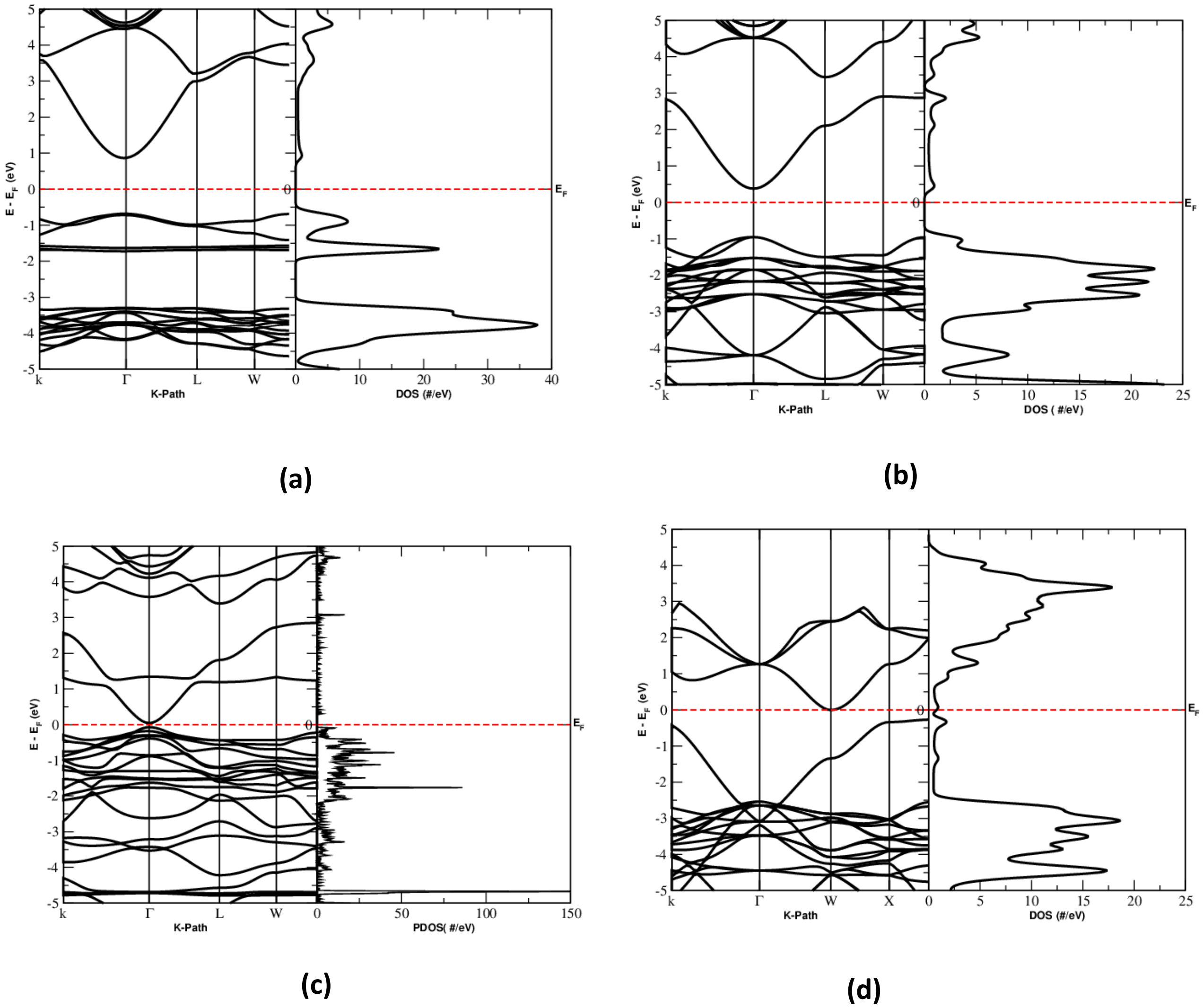

(a)

(b)

(c)

(d)

Figure 1: Energy band structures with DoS for all studied perovskites. (a) X = F, (b) X= Cl, (c) X=Br and (d) X = I

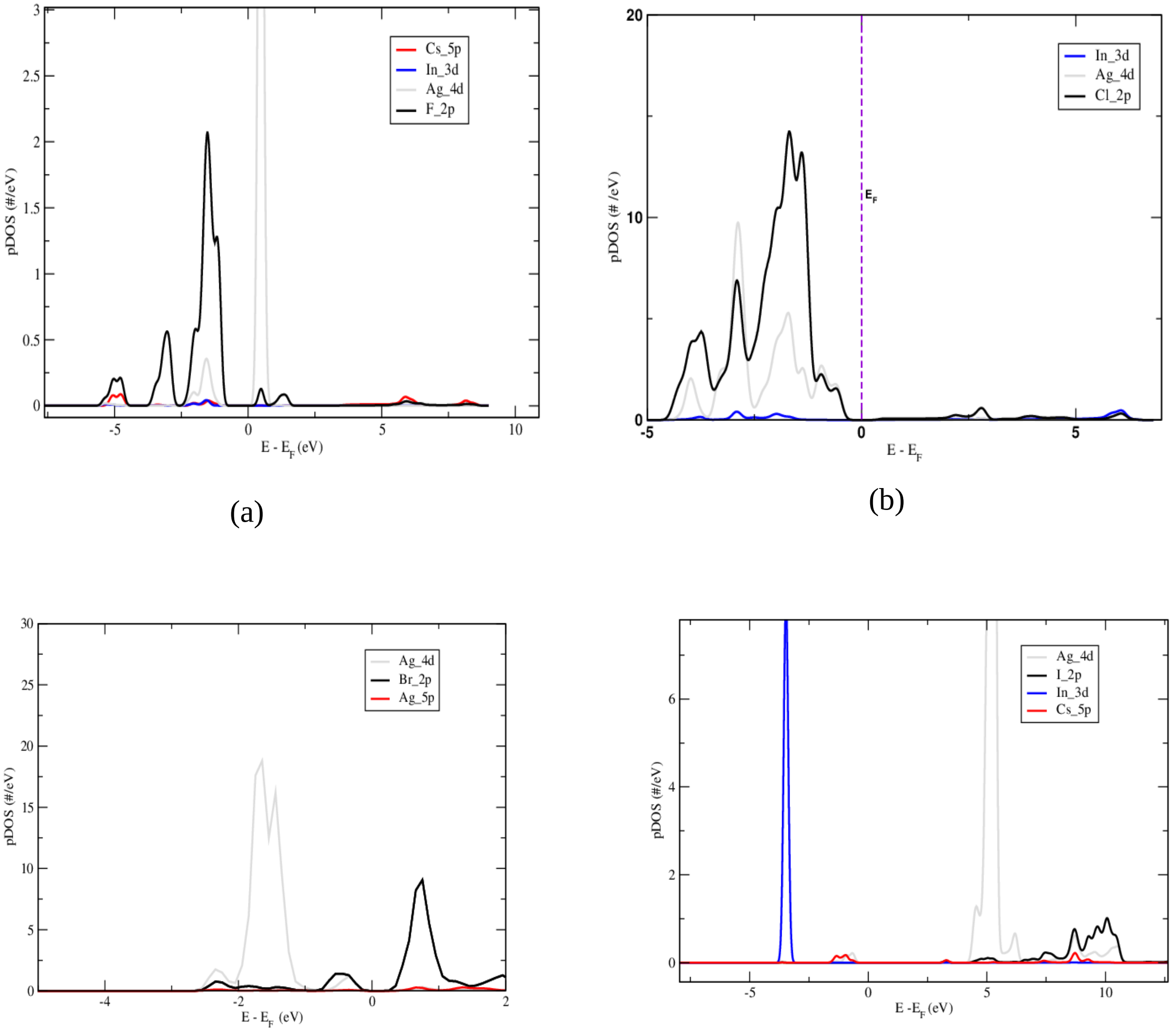

(a) (b)

(c) (d)

Figure 2: Projected DOS plots for (a) Cs_2InAgF_6 , (b) $Cs_2InAgCl_6$, (c) $Cs_2InAgBr_6$ (d) Cs_2InAgI_6

4.0 DISCUSSION

All crystals were first relaxed to determine their equilibrium lattice parameters. It can be seen from Table 1 that compared to the lattice constants of the respective material reported by the indicated references, the calculated values can be said to be in fair agreement, deviating only in a narrow range of +0.16% to +1.7%. As expected, it can be seen from the table that the calculated cell sizes increase as the halide atom changes from Fluorine to Iodine (i.e. down the periodic table). The bulk moduli of the perovskite material were also calculated in order to understand their mechanical properties. Bulk modulus measures the ease or resistance to volume changes (brittleness) whilst the ease of change in shape is measured by the shear modulus. The ratio of the bulk to the shear modulus, called the Pugh ratio is a measure of the ductile nature of the material. A Material is classified as ductile if its Pugh ratio is greater than 1.75 whilst the Poisson ratio should be greater than 0.26 (Waqas Mukhtar et al., 2021). Poisson's ratio is the ratio of the change in the width per unit width of a material, to the change in its length per unit length, as a result of strain.

The values of bulk moduli shown in Table 1 are similar to those obtained by Tariq *et al* (see Table 1 of (M. Tariq, Malak Azmat Ali, A. Laref, 2020). In particular for X = F, the values of bulk modulus was a match to earlier reported values (see Table 1 of (Sandeep et al., 2017)) giving confidence to our results. Except for X= I, all Pugh ratios are greater than 1.75 and would therefore be ductile in nature implying they would have a fair degree of flexibility which is suitable for solid state and flexible electronic applications. A Material is expected to form stable double perovskite if its tolerance value is in the range $0.8 \leq t \leq 1$ and its octahedral factor is greater 0.41 (Volonakis et al., 2017) or more precisely in the range $0.4 < t \leq 0.9$ (Meyer et al., 2018). The tolerance values and octahedral factors for the material, included in Table 1, are within the stability ranges. From these values it appears that all the materials studied would form stably as double perovskite crystals although the octahedral factor decreases as the ion X gets larger. The observation suggests that larger anions would least form as double perovskites.

The mechanical stability of the perovskite material was further assessed by determining whether they met the following conditions (for stability)(Bouafia et al., 2015): $|C_{44}| > 0$, $C_{11} - |C_{12}| > 0$ and $C_{11} + |C_{12}| > 0$. The results of the comparisons for all the compounds as displayed in Table 2 indicates that by this criterion alone all but for X = F are mechanically stable under reasonable stress.

The apparent conflict in the observation that all the studied material would form double perovskites yet Table 2 shows that for X = F, $C_{44} < 0$, can only be resolved by making a distinction between formation as double perovskite crystals and existing stably as such. For X=F, a hypothetical double perovskite may form but is not expected to exhibit stable mechanical properties.

4.1 Electronic properties

The electronic properties of the material is summarized in Figure 1 by the band structure and distribution of density of states. The band gap values derived from calculations are shown in Table 3. Values from other works are also indicated for comparison. Except for Cs_2InAgI_6, (which by the band structure, appears to be an indirect band gap material) the conduction band minima (CBM) and the valence band maxima (VBM) for all the compounds occur at the $\Gamma -$ point of the Brillouin zone, making them direct bandgap crystals. The indirect bandgap of Cs_2InAgI_6 indicates that it is not a good candidate perovskite for PVCs. Particularly noticeable is the very small energy band gap value for $Cs_2InAgBr_6$ which is consistent with the value reported earlier (Z. Zhang, J. Su, J. Hou, Z. Lin, Z. Hu, J. Chang, J. Zhang, 2019). This band gap value would make $Cs_2InAgBr_6$ electronically unsuitable particularly for solar energy harvesting. For X =Br, the double perovskite material may thus be considered for bandgap engineering. Of the three direct bandgap perovskites studied, $Cs_2InAgCl_6$ appears to offer the most promising electronic property with an energy bandgap of 1.5 eV.

Although an experimental band gap value of 3.3 eV has been reported, our value of 1.5 eV is consistent with several other calculations. (Z. Zhou, M.S. Xia, X. Molokeev, D. Peng Zhang, 2017) (Wonseok Lee, Seunghwa Hong, 2019). Projected partial densities of state, pDOS, plots show that across all the materials studied, the *2p* orbitals of the X anions dominate near their Fermi levels with the *4d* orbitals of the Ag cation (see Fig. 2) being the other most significant contributor of electrons to similar that energy band which is important to semiconducting properties. For clarity, other orbitals were left out of the plot as they were too small to be shown on the scale.

5.0 CONCLUSION

The mechanical stability of Pb-free double perovskites Cs_2InAgX_6 (X = halides F, Cl, Br, I) were studied along with their suitability, electronically, for photovoltaic cells. The results suggests that except for X = I, all perovskites in the series are direct bandgap semiconductors, but the bandgap for X = Br is so small that it is not good for PVC applications. Except for X = I, all material studied were found to be malleable. Results from the study shows that $Cs_2InAgCl_6$ would have the desired bandgap for PVC candidate material, and would be the most mechanically stable candidate among the series of halide double perovskites studied.

REFERENCES

A. Kaltzoglou, D. Perganti, M. Antoniadou, A.G. Kontos, P. F. (2016). Stress tests on Hole-transporting, dye-sensitized solar cells with the Cs2SnI6 defect perovskite as material. , *Energy Procedia*, *102*, 49–55.

A.E. Maughan, A.M. Ganose, M.A. Almaker, D.O. Scanlon, J. R. N. (2018). Tolerance factor and cooperative tilting effects in vacancy-ordered double perovskite halides. *Chem. Mater.*, *30*, 3909–3919.

Amal Moussali, Mahdad Benzardjab Amina, Benattou Fassi, Ibrahim Ameri, Mohammed Ameri, Y. A.-D. (2020). First-principles calculations to investigate structural and thermodynamic properties of Ni2LaZ (Z = As, Sb and Bi) Heusler alloys. *Indian Journal of Physics*, *94*, 1733–1747.

Bouafia, H., Sahli, B., Hiadsi, S., Abidri, B., Rached, D., Akriche, A., & Mesli, M. N. (2015). Theoretical investigation of structural, elastic, electronic, and thermal properties of KCaF3, K0.5Na0.5CaF3 and NaCaF3 Perovskites. *Superlattices and Microstructures*, *82*, 525–537. https://doi.org/10.1016/j.spmi.2015.03.004

Christopher N. Savory, Aron Walsh, and D. O. S. (2016). Can Pb-Free Halide Double Perovskites Support High-Efficiency Solar Cells? *ACS Energy Lett.*, *1*, 949–955.

D. Shi, V. Adinolfi, R. Comin, M. Yuan, E. Alarousu, A. Buin, Y. Chen, S. H., & A. Rothenberger, K. K. (2015). Low trap-state density and long carrier diffusion in organolead trihalide perovskite single crystals. *Science*, *347*, 519–522.

Enamul Haque, M. A. H. (2019). Electronic, phonon transport and thermoelectric properties of Cs2InAgCl6 from first-principles study. *Computational Condensed Matter*, *16*(e00374).

Erum, N., & Iqbal, M. A. (2016). First Principles Investigation of Fluorine Based Strontium Series of Perovskites. *Communications in Theoretical Physics*, *66*(5), 571–578. https://doi.org/10.1088/0253-6102/66/5/571

Filip, M. R.; Hillman, S.; Haghighirad, A. A.; Snaith, H. J.; Giustino, F. (2016). Band Gaps of Lead-Free Halide double perovskites Cs2BiAgCl6 and Cs2BiAgBr6 from theory and experiment. *J. Phys. Chem. Lett.*, *7*, 2579–2585.

G. Volonakis, F. G. (2018). No Title. *Appl. Phys. Lett.*, *112*, 243901.

Green, M. A., Ho-Baillie, A., & Snaith, H. J. (2014). The emergence of perovskite solar cells. *Nature Photonics*, *8*(7), 506–514. https://doi.org/10.1038/nphoton.2014.134

H.-S. Kim, C.-R. Lee, J.-H. Im, K.-B. Lee, T. Moehl, A. Marchioro, S.-J. M., & R. Humphry-Baker, J.-H. Yum, J. E. (2012). Lead Iodide Perovskite Sensitized All-Solid-State Submicron Thin Film Mesoscopic Solar Cell with Efficiency Exceeding 9%. . . *Moser, Sci. Rep*, *2*, 1–7.

Hang Yin, Yeming Xian, Yongli Zhang, Wenzhe Li, J. F. (2019). Structurally Stabilizing and Environment Friendly Triggers: Double-Metallic Lead-Free Perovskites. *Solar RRL*, *3*(9). https://doi.org/https://doi.org/10.1002/solr.201900148

J. H. Noh, S. H Im, J. H Heo, T. N Mandal, S. I. S. (2013). Chemical management for colorful, efficient, and stable inorganic–organic hybrid nanostructured solar cells. *Nano Letters*, *13*.

J. Zhou, J. Luo, X. Rong, P. Wei, M.S. Molokeev, Y. Huang, J. Zhao, Q. L., & X. Zhang, J. Tang, Z. X. (2019). Lead-free perovskite derivative Cs2SnCl6-xBrx single crystals for narrowband Photodetectors. *Adv. Optical Mater.*, *1*, 1900139.

Li, L., Wang, Y. J., Liu, D. X., Ma, C. G., Brik, M. G., Suchocki, A., Piasecki, M., & Reshak, A. H. (2017). Comparative first-principles calculations of the electronic, optical, elastic and thermodynamic properties of XCaF3 (X = K, Rb, Cs) cubic perovskites. *Materials Chemistry and Physics*, *188*, 39–48. https://doi.org/10.1016/j.matchemphys.2016.12.033

Lv, Z. L., Cui, H. L., Wang, H., Li, X. H., & Ji, G. F. (2016). Electronic and elastic properties of BaLiF3 with pressure effects: First-principles study. *Physica Status Solidi (B) Basic Research*, *253*(9), 1788–1794. https://doi.org/10.1002/pssb.201600094

M. Tariq, Malak Azmat Ali, A. Laref, G. M. (2020). Anion replacement effect on the physical properties of metal halide double perovskites Cs2AgInX6 (X¼F, Cl, Br, I). *Solid State Communications*, *113929*, 314–315.

Mathew, N. P., Kumar, N. R., & Radhakrishnan, R. (2019). First principle study of the structural and optoelectronic properties of direct bandgap double perovskite Cs2AgInCl6. *Materials Today: Proceedings*, *33*, 1252–1256. https://doi.org/10.1016/j.matpr.2020.03.489

Meyer, E., Mutukwa, D., Zingwe, N., & Taziwa, R. (2018). Lead-free halide double perovskites: A review of the structural, optical, and stability properties as well as their viability to replace lead halide perovskites. *Metals*, *8*(9). https://doi.org/10.3390/met8090667.

Michael M. Lee, Joël Teuschertsutomu, M. N. M. H. J. S. (2012). Efficient Hybrid Solar Cells Based on Meso-Superstructured Organometal Halide Perovskites. *Science*, *338*, 643–647.

N.K. Noel, S.D. Stranks, A. Abate, C. Wehrenfennig, S. Guarnera, A. A. H., & Petrozza, A. (2014). No. *Energy Environ. Sci.*, *7*(9), 3061–3068.

Nam Joong Jeon, Jun Hong Noh, Woon Seok Yang, Young Chan Kim, Seungchan Ryu, J. S. & S. I. S. (2015). Compositional engineering of perovskite materials for high-performance solar cells. *Nature*, *517*, 476–480.

Nayak, P. K., Mahesh, S., Snaith, H. J., Cahen, D. (2019). Photovoltaic solar cell technologies: analysing the state of the art. *Nature Reviews Materials*, *4*(4), 269–285. https://doi.org/10.1038/s41578-019-0097-0

NREL. (2022). *Best Research-Cell Efficiency Chart*. https://www.nrel.gov/pv/cell-efficiency.html

P.K. Kung, M.H. Li, P.Y. Lin, J.Y. Jhang, M. Pantaler, D.C. Lupascu, G. Grancini, P. C. (2020). Lead-free double perovskites for perovskite solar cells. *Sol RRL*, 190030.

P Giannozzi, S Baroni, N. B. et al. (2017). QUANTUM ESPRESSO: a modular and open-source software project for quantum simulations of materials. *J. Phys.:Condens. Matter*, *29*(465901).

Q. Dong, Y. Fang, Y. Shao, P. Mulligan, J. Qiu, L. Cao, J. H. (2015). Electron-hole diffusion lengths > 175 μm in solution-grown CH3NH3PbI3 single crystals. *Science*, *347*, 967–970.

S.D. Stranks, G.E. Eperon, G. Grancini, C. Menelaou, M.J. Alcocer, T. Leijtens, L., & M. Herz, A. P. (2013). Electron-hole diffusion lengths exceeding 1 micrometer in an organometal trihalide perovskite absorber. *Science*.

Sandeep, Rai, D. P., Shankar, A., Ghimire, M. P., Khenata, R., Bin Omran, S., Syrotyuk, S. V., & Thapa, R. K. (2017). Investigation of the structural, electronic and optical properties of the cubic RbMF3 perovskites (M = Be, Mg, Ca, Sr and Ba) using modified Becke-Johnson exchange potential. *Materials Chemistry and Physics*, *192*, 282–290. https://doi.org/10.1016/j.matchemphys.2017.02.005

Slavney, A. H.; Hu, T.; Lindenberg, A. M.; Karunadasa, H. I. A. (2016). Bismuth-Halide Double Perovskite with Long Carrier Recombination Lifetime for Photovoltaic Applications. *J. Am. Chem. Soc.*, *138*(2138–2141).

T.J. Jacobsson, M. Pazoki, A. Hagfeldt, T. E. (2015). Goldschmidt’s Rules and Strontium Replacement in Lead Halogen Perovskite Solar Cells: Theory and Preliminary Experiments on CH3NH3SrI3. *J. Phys. Chem C*, *119*, 25673–25683.

Volonakis, G., Haghighirad, A. A., Milot, R. L., Sio, W. H., Filip, M. R., Wenger, B., Johnston, M. B., Herz, L. M., Snaith, H. J., & Giustino, F. (2017). Cs2InAgCl6: A New Lead-Free Halide Double Perovskite with Direct Band Gap. *Journal of Physical Chemistry Letters*, *8*(4), 772–778. https://doi.org/10.1021/acs.jpclett.6b02682

W. Khan, S. Azam, M.B. Kanoun, S. G.-S. (2016). Optoelectronic structure and related transport properties of BiCuSeO-based oxychalcogenides: First principle calculations. *Solid State Sciences, 58*.

Waqas Mukhtar, M., Ramzan, M., Rashid, M., Naz, G., Imran, M., Fahim, F., AlObaid, A. A., Al-Muhimeed, T. I., & Mahmood, Q. (2021). New lead-free double perovskites A2NaInI6 (A = Cs, Rb) for solar cells and renewable energy; first principles analysis. *Materials Science and Engineering B: Solid-State Materials for Advanced Technology*, *273*(July), 115420. https://doi.org/10.1016/j.mseb.2021.115420

Wonseok Lee, Seunghwa Hong, S. K. (2019). J. Phys. Chem. C. *J. Phys. Chem. C*, *123*, 2665–2672.

Xin-Gang Zhao, Dongwen Yang, Yuanhui Sun, Tianshu Li†, Lijun Zhang, Liping Yu, and A. Z. (2017). Cu–In Halide Perovskite Solar Absorbers. *J. Am. Chem. Soc.*, *139*, 6718–6725.

Z. Zhang, J. Su, J. Hou, Z. Lin, Z. Hu, J. Chang, J. Zhang, Y. H. (2019). No Title. *J. Phys. Chem. Lett.*, *10*, 1120–1125.

Z. Zhou, M.S. Xia, X. Molokeev, D. Peng Zhang, Q. L. (2017). No Title. *J. Mater. Chem. A*, *5*, 15031–15037.

Zhen Li, Mengjin Yang, Ji-Sang Park, Su-Huai Wei, Joseph J. Berry, and K. Z. (2016). Stabilizing Perovskite Structures by Tuning Tolerance Factor: Formation of Formamidinium and Cesium Lead Iodide Solid-State Alloys. *Chem. Mater*, *28*, 284–292.